Journal of Pioneering Medical Sciences
Received January 15, 2024 Accept June 01, 2024 Publish June 30, 2024.
Volume 13, Issue 3, Pages 66-74

DOI https://doi.org/10.61091/jpms202413311

Theoretical Analysis and Numerical Simulation of the Transmission Dynamics of Monkeypox Virus: A Common Disease in Central and West Africa

Fazal Dayan[1], Muhammad Aziz ur Rehman[1], Abaid ur Rehman Virk[1,*] and Samiullah Salim[1]
[1]Department of Mathematics, School of Science University of Management and Technology Lahore 5400 Pakistan.

Corresponding author: Abaid ur Rehman Virk (e-mail: abaidrehman@umt.edu.pk).

Abstract Monkeypox (MPX), which is similar to smallpox and cowpox, is caused by the MPX virus. It primarily appears in isolated areas in Central and West Africa, often near tropical rainforests. In this paper, a mathematical model of the MPX virus is explored and the sensitivity of the reproduction number is investigated. Two different numerical techniques, forward Euler, and nonstandard finite difference (NSFD) are constructed for solving the studied model numerically. The convergence, positivity, boundedness, and consistency of the NSFD scheme are investigated. The simulated graphs are displayed to illustrate the main attributes of the developed methodologies. The simulation results indicate that the NSFD scheme demonstrates unconditional convergence, whereas the convergence of the other two techniques is contingent upon the values of the step sizes.

Key Words Monkeypox Virus, nonstandard finite difference, convergence, boundedness, consistency, positivity

1. Introduction

Monkeypox, or MPX, arises from infection with the MPX virus. It is a viral ailment capable of transmission between individuals and sporadically from contaminated surfaces and objects handled by an infected person. Additionally, in environments where the MPX virus circulates among certain wildlife species, transmission can occur from infected animals to humans through direct contact. Resembling smallpox in its clinical presentation, this illness predominantly affects Central and West Africa, with occasional outbreaks in other regions. The MPX virus was initially identified in Denmark in 1958, within monkeys housed for research purposes. The earliest documented human case of MPX occurred in the Democratic Republic of the Congo (DRC) in 1970, involving a nine-month-old boy. The young boy suffered from an illness resembling smallpox, from which a virus similar to MPXV was identified [1]–[6]. Between October 1970 and May 1971, six instances of human MPXV were documented in Liberia, Nigeria, and Sierra Leone. The initial case of MPXV in Nigeria was noted in 1971, with 10 additional cases reported between 1971 and 1978. Subsequently, thousands of human MPX cases have been verified across 15 nations, including 11 within Africa. MPX was introduced to countries such as the United Kingdom, the USA, Israel, and Singapore [7], [8].

Since its initial identification, MPX has been documented in humans across various Central and West African nations, including Nigeria, Cameroon, Gabon, Liberia, Central African Republic, Congo, South Sudan, and Sierra Leone. Notably, a 2003 outbreak in the United States marked the first occurrence of MPX infections in humans outside of Africa. Additionally, several non-African countries, such as the UK, Israel, and Singapore, have reported imported cases of MPX from Africa. In May 2022, several European and North American countries, including Italy, France, Germany, Sweden, Spain, Portugal, Australia, Canada, and Belgium, reported confirmed cases of MPX with no direct epidemiological linkage to Africa [3]. As of April 23, 2024, there have been a cumulative total of 95,340 confirmed cases of MPXV worldwide, comprising 92,590 cases in non-endemic regions (countries with no historical cases reported) and 2,750 cases in endemic regions (countries with a history of reported cases). The total number of deaths attributed to MPX virus stands at 184 [9].

MPX can manifest with a spectrum of signs and symptoms. While some individuals may experience milder manifestations, others may develop severe illness requiring medical attention in a healthcare setting. Those particularly vulnerable to experiencing more severe symptoms typicallyinclude pregnant individuals, children, and immunocompro-

mised persons, such as those with untreated and advanced HIV infection. Typical symptoms of MPX encompass a rash persisting for 2–4 weeks, often accompanied by fever, headache, muscle aches, back pain, fatigue, and swollen lymph nodes. The rash, resembling blisters or sores, can manifest on various body parts including the face, palms, soles, groin, genital and anal regions. Additionally, lesions may occur in the oral cavity, throat, anus, rectum, vagina, or eyes. The quantity of sores can vary from singular to numerous. In some cases, individuals may experience inflammation within the rectum (proctitis) leading to intense pain, and inflammation of the genital region resulting in urinary difficulties [1].

The primary reservoir for MPX virus infection in humans remains unidentified, although various studies have indicated that animals, particularly rodents and non-human primates, are likely reservoirs for the virus [10]. Currently, there are no established treatments for MPX infection; however, several innovative antiviral drugs, such as Brincidofovir, Tecovirimat, and vaccinia immune globulin, are available to manage disease spread. The past decade has witnessed a notable rise in MPX cases, linked to the decline in herd immunity against smallpox. Although smallpox vaccination boasts an 85 percent success rate in preventing MPX, its routine availability has ceased following global smallpox eradication. Nevertheless, post-exposure vaccination can assist in averting or reducing the severity of the disease [11], [12].

An infectious disease is a sickness that likely would not have occurred without the introduction of an infectious microorganism. However, not all microorganisms associated with illness cause a recognizable disease. When a parasite has the potential to cause damage to its host, it is known as a pathogen. The term 'parasite' generally refers to organisms that belong to the virus, bacteria, and fungi or multicellular organisms which include helminths and arthropods. Most infections are subclinical, in which the symptoms are so mild that the infected person does not seek medical attention. However, the agent can still be transferred to others during this early stage. Epidemiology is the science of understanding the patterns of disease occurrence in populations and what can be done about them. This is most commonly illustrated by infections (or infestations) and toxic diseases; non-infectious constitutional diseases such as diabetes or cancer were traditionally thought to be beyond the scope of epidemiologists but are now embraced, e.g. through nutrition studies of coronary heart disease. The role of mathematical modeling is best realized considering the interest in providing a mathematical pattern of the incidence of mathematical models participating in the data collection process. It is of great value during periods of post-epidemic data collection by helping to interpret the observed disease dynamics.

Mathematical models are now considered to be an essential tool for the study of infectious diseases. They provide an important means of understanding the control of infectious diseases by assessing the impact of possible interventions. The aim of infectious disease modelling is to provide an integrated approach to epidemiological and dynamical understanding of transmission dynamics for control purposes. The modelling of epidemics has a long history, but the use of mathematical models has increased in recent years. Infectious diseases are now recognized as a frequent threat to society and the economy. The threat can come from a variety of sources, including well-known diseases like influenza, and diseases that are ancient, like tuberculosis, or emerging, like HIV or the new variant Creutzfeldt-Jakob disease. Many models have now been developed for well-known infectious diseases, including many zoonotic infections like Rabies and West Nile virus, which may lead to dramatic human epidemics.

Mathematical modelling is a set of techniques that are useful in managing and evaluating uncertainties and in minimizing the risks associated with the development and use of a variety of technological systems. Mathematical modelling requires a theoretical statement of the probable processes generating completely or partially scored distributions for use in the management analysis process. A model manifestation is a version of the model defined precisely enough that it can be either implemented in a computational system or laid out as a plan or statement that can be carried out manually. When the model manifestation is implemented and normalized, it becomes a model program, which can be executed and the results understood by a user to whom the results are exposed. Epidemiologic considerations today contribute information to programs of infection control, mass childhood vaccination, and the global picture of the HIV pandemic. Epidemiology evidence that is only qualitative offers the potential of describing the processes and the variables implicated in the problem situation at hand.

In the past, the disease has been largely overlooked, resulting in limited knowledge about how it spreads. Nevertheless, a few studies have attempted to investigate the dynamics of the MPX virus using mathematical modeling techniques. Bhunu et al. formulated a mathematical model to depict the transmission dynamics of MPX [13]. Somma et al. introduced a mathematical model illustrating the transmission dynamics of the MPX virus, involving two interacting host populations: humans and rodents. Within the human population, parameters such as the quarantine class and public enlightenment campaign were integrated to control disease spread [14]. Usman and Adamu constructed a mathematical model to analyze the dynamics of MPX virus transmission, integrating control strategies that combine vaccination and treatment interventions [15].

Philemon developed novel compartmental models, taking into account factors such as quarantine measures, congenital infection, and various epidemiological aspects [16]. Samuel et al. examined the cross-sectional prevalence of people with healed deformities from pox recovery and those with active pox infection using four longitudinal studies and generalized linear models [17]. Peter et al. developed and analyzed a compartmental mathematical model that included isolation and quarantine compartments and represented the dynamics

of MPX [18], [19]. To understand the dynamics of MPX, Khan et al. presented a mathematical model that included two forms of transmission: cross-infection between people and animals and horizontal dispersion among humans [20]. Al-Shomrani et al. investigated the transmission dynamics of the MPX virus using an SEIR-based deterministic model that included elements such as the prodromal stage, fluctuating infectivity, and hospitalization [21]. Peter et al. investigated a deterministic mathematical model of the MPX virus [22]. Cadmus et al. followed the PRISMA guidelines to perform a systematic review and meta-analysis of existing data on MPX in Nigeria [23]. Onitilo et al. [24] developed a deterministic model to depict the dynamics of MPX transmission in response to quarantine restrictions and public education. To examine potential outbreaks in the United States, a deterministic mathematical model of the MPX virus is developed using complex, fractional, and classical differential equations [25]. The transmission dynamics of MPX virus epidemics in the United States are investigated using a mechanistic model that depicts the interaction of several groups of people, reflecting various infection phases and hospitalization processes [26].

R.E. Mickens [27] developed the NSFD method, which has become one of the most effective techniques in recent years. Researchers have successfully solved a variety of differential equations using NSFD methodologies [28]–[34], to name a few. Verma and Kayenat used the NSFD method to study the generalized Burgers-Huxley (GBH) equation [35].

The purpose of this work is to investigate an effective implicit numerical integration technique for dealing with the MPX disease. Two numerical methods, forward Euler and NSFD, are developed to solve the examined problem. The convergence, positivity, boundedness, and consistency of the NSFD scheme are investigated. Numerical simulations are used in this work to verify the outcomes of analytical computations. The proposed implicit numerical integration scheme's tool is effective, and it incorporates all of the dynamical qualities required for long-term disease behavior. The primary goal of this study is to identify an efficient implicit numerical integration technique for addressing the MPX disease model. To solve the studied model, two numerical algorithms—forward Euler and NSFD—are developed. We thoroughly investigate the NSFD scheme's positivity, boundedness, and consistency. This work uses numerical simulations to validate the results of analytical computations. The results show that the suggested implicit numerical integration approach is trustworthy, efficient, and includes all of the dynamic properties required to capture long-term illness behavior.

2. Monkeypox Virus Model

We consider the model discussed by [22].

$$\frac{dS_h}{dt} = \theta_h - \frac{(\beta_1 I_r + \beta_2 I_h)S_h}{N_h} - \mu_h S_h + \phi Q_h, \quad (1)$$

$$\frac{dE_h}{dt} = \frac{(\beta_1 I_r + \beta_2 I_h)S_h}{N_h} - (\alpha_1 + \alpha_2 + \mu_h)E_h, \quad (2)$$

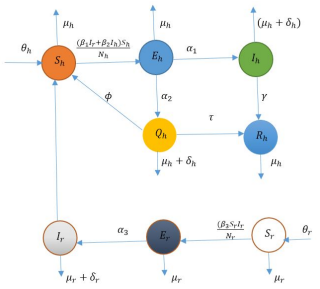

Figure 1: Flowchart of the model

Variables	Description
S_h	Population of susceptible
I_h	Population of infected humans
Q_h	Population of isolated humans
R_h	Population of recovered humans
S_r	Population of susceptible rodents
E_r	Population of exposed rodents
I_r	Population of infected rodents

Table 1: Details of the model variables

$$\frac{dI_h}{dt} = \alpha_1 E_h - (\mu_h + \delta_h + \gamma)I_h, \quad (3)$$

$$\frac{dQ_h}{dt} = \alpha_2 E_h - (\phi + \tau + \mu_h + \delta_h)Q_h, \quad (4)$$

$$\frac{dR_h}{dt} = \gamma I_h + \tau Q_h - \mu_h R_h, \quad (5)$$

$$\frac{dS_r}{dt} = \theta_r - \frac{\beta_3 S_r I_r}{N_r} - \mu_r S_r, \quad (6)$$

$$\frac{dE_r}{dt} = \frac{\beta_3 S_r I_r}{N_r} - (\mu_r + \alpha_3)\, E_r, \quad (7)$$

$$\frac{dI_r}{dt} = \alpha_3\, E_r - (\mu_r + \delta_r)\, I_r. \quad (8)$$

The parameters and variables used above are described in Table 1 and Table 2 respectively. Figure 1 shows the flowchart of the above model.

System (1-8) has a disease-free equilibrium (DFE) $P_0 = (\frac{\theta_h}{\mu_h},\ 0,\ 0,\ 0\ ,\ 0,\ \frac{\theta_r}{\mu_r}\ ,\ 0,\ 0)$ and an endemic equilibrium (EE)

Parameters	Description
$\theta_h)$	Rate of human recruitment
$\theta_r)$	Rate of rodent recruitment
$\beta_1)$	Rate of rodent-to-human contact
$\beta_2)$	Rate of human-to-human contact
$\beta_3)$	Rate of rodent-to-rodent contact
$\alpha_1)$	The proportion of exposed humans becoming infected
$\alpha_2)$	Proportion identified as suspected cases
$\varphi)$	Proportion remaining undetected after diagnosis
$\tau)$	Rate of progression from isolation to recovery
$\gamma)$	Rate of human recovery
$\mu_h)$	Rate of natural human mortality
$\mu_r)$	Rate of natural rodent mortality
$\delta_r)$	Rate of rodent mortality due to disease
$\delta_h)$	Rate of human mortality due to disease

Table 2: Details of the model parameter

$P_1 = (S_h{}^*, E_h{}^*, I_h{}^*, Q_h{}^*, R_h{}^*, S_r{}^*, E_r{}^*, I_r{}^*)$. The basic reproduction number for the studied model is

$$R_0 = \frac{\beta_2\alpha_1}{(\alpha_1+\alpha_2+\mu_h)(\mu_h+\delta_h+\gamma)}.$$

A. *Sensitivity of* R_0

The sensitivity analysis evaluates how changes in an independent variable affect a specific dependent variable within a given set of assumptions [36]. A negative sensitivity index denotes an inverse relationship between the parameter and R_0, while a positive sensitivity index indicates that increasing the parameter value leads to an increase in R_0. We used the following expression to determine the sensitivity of a parameter ζ

$\xi(\zeta) = \frac{\zeta}{\mathrm{R}_o}\frac{\partial}{\partial\zeta}(R_0)$.

$$\xi(\beta_2) = \frac{\beta_2}{R_0}\cdot\frac{dR_0}{d\beta_2} = \frac{\beta_2}{\frac{\beta_2\alpha_1}{(\alpha_1+\alpha_2+\mu_h)(\mu_h+\delta_h+\gamma)}}\cdot\frac{d\left(\frac{\beta_2\alpha_1}{(\alpha_1+\alpha_2+\mu_h)(\mu_h+\delta_h+\gamma)}\right)}{d\beta_2} = 1.$$

$$\xi(\alpha_1) = \frac{\alpha_1}{R_0}\cdot\frac{dR_0}{d\alpha_1} = \frac{\alpha_1}{\frac{\beta_2\alpha_1}{(\alpha_1+\alpha_2+\mu_h)(\mu_h+\delta_h+\gamma)}}\cdot\frac{d\left(\frac{\beta_2\alpha_1}{(\alpha_1+\alpha_2+\mu_h)(\mu_h+\delta_h+\gamma)}\right)}{d\alpha_1} = 1.$$

$$\xi(\alpha_2) = \frac{\alpha_2}{R_0}\cdot\frac{dR_0}{d\alpha_2} = \frac{\alpha_2}{\frac{\beta_2\alpha_1}{(\alpha_1+\alpha_2+\mu_h)(\mu_h+\delta_h+\gamma)}}\cdot\frac{d\left(\frac{\beta_2\alpha_1}{(\alpha_1+\alpha_2+\mu_h)(\mu_h+\delta_h+\gamma)}\right)}{d\alpha_2} = \frac{-(\beta_2\alpha_1)(\mu_h+\delta_h+\gamma)}{((\alpha_1+\alpha_2+\mu_h)(\mu_h+\delta_h+\gamma))^2}.$$

$$\xi(\gamma) = \frac{\gamma}{R_0}\cdot\frac{dR_0}{d\gamma} = \frac{\gamma}{\frac{\beta_2\alpha_1}{(\alpha_1+\alpha_2+\mu_h)(\mu_h+\delta_h+\gamma)}}\cdot\frac{d\left(\frac{\beta_2\alpha_1}{(\alpha_1+\alpha_2+\mu_h)(\mu_h+\delta_h+\gamma)}\right)}{d\gamma} = \frac{-(\beta_2\alpha_1)(\alpha_1+\alpha_2+\mu_h)}{((\alpha_1+\alpha_2+\mu_h)(\mu_h+\delta_h+\gamma))^2}.$$

$$\xi(\mu_h) = \frac{\mu_h}{R_0}\cdot\frac{dR_0}{d\mu_h} = \frac{\mu_h}{\frac{\beta_2\alpha_1}{(\alpha_1+\alpha_2+\mu_h)(\mu_h+\delta_h+\gamma)}}\cdot\frac{d\left(\frac{\beta_2\alpha_1}{(\alpha_1+\alpha_2+\mu_h)(\mu_h+\delta_h+\gamma)}\right)}{d\mu_h} = \frac{-(\beta_2\alpha_1)(\alpha_1+\alpha_2+\delta_h+\gamma+2\mu_h)}{((\alpha_1+\alpha_2+\mu_h)(\mu_h+\delta_h+\gamma))^2}.$$

The calculated findings indicate that β_2 and α_1 are sensitive parameters. Increasing sensitive parameters increases R_0, and vice versa.

3. Numerical Modelling

In this section, we will develop two different numerical schemes for the solution of the studied model.

A. *Forward Euler Method*

Considering the system (1-8), we develop a forward Euler scheme. Constructing a numerical scheme for the forward Euler involves making the following supposition.

$S_h(t) \approx {S_h}^n, E_h(t) \approx {E_h}^n, I_h(t) \approx {I_h}^n, Q_h(t) \approx {Q_h}^n, R_h(t) \approx {R_h}^n, S_r(t) \approx {S_r}^n, E_r(t) \approx {E_r}^n$ and $I_r(t) \approx {I_r}^n$.

$${S_h}^{n+1} = {S_h}^n + h\left(\theta_h - \frac{(\beta_1{I_r}^n+\beta_2{I_h}^n){S_h}^n}{N_h} - \mu_h{S_h}^n + \varphi{Q_h}^n\right), \quad (9)$$

$${E_h}^{n+1} = {E_h}^n + h\left(\frac{(\beta_1{I_r}^n+\beta_2{I_h}^n){S_h}^n}{N_h} - (\alpha_1+\alpha_2+\mu_h){E_h}^n\right), \quad (10)$$

$${I_h}^{n+1} = {I_h}^n + h\left(\alpha_1{E_h}^n - (\mu_h+\delta_h+\gamma){I_h}^n\right), \quad (11)$$

$${Q_h}^{n+1} = {Q_h}^n + h\left(\alpha_2{E_h}^n - (\varphi+\tau+\mu_h+\delta_h){Q_h}^n\right), \quad (12)$$

$${R_h}^{n+1} = {R_h}^n + h\left(\gamma{I_h}^n + \tau{Q_h}^n - \mu_h{R_h}^n\right), \quad (13)$$

$${S_r}^{n+1} = {S_r}^n + h(\theta_r - \frac{\beta_3{S_r}^n{I_r}^n}{N_r} - \mu_r{S_r}^n), \quad (14)$$

$${E_r}^{n+1} = {E_r}^n + h\left(\frac{\beta_3{S_r}^n{I_r}^n}{N_r} - (\mu_r+\alpha_3){E_r}^h\right), \quad (15)$$

$${I_r}^{n+1} = {I_r}^n + h\left(\alpha_3{E_r}^n - (\mu_r+\delta_r){I_r}^n\right). \quad (16)$$

B. *NSFD Scheme*

$${S_h}^{n+1} = \frac{{S_h}^n N_h + hN_h(\varphi{Q_h}^n + \theta_h)}{N_h + h\mu_h N_h + h(\beta_1{I_r}^n + \beta_2{I_h}^n)}, \quad (17)$$

$${E_h}^{n+1} = \frac{N_h{E_h}^n + h(\beta_1{I_r}^n + \beta_2{I_h}^n){S_h}^n}{N_h(1+h(\alpha_1+\alpha_2+\mu_h))}, \quad (18)$$

$${I_h}^{n+1} = \frac{{I_h}^n + h\alpha_1{E_h}^n}{1+h(\mu_h+\delta_h+\gamma)}, \quad (19)$$

$${Q_h}^{n+1} = \frac{{Q_h}^n + h\alpha_2{E_h}^n}{1+h(\varphi+\tau+\mu_h+\delta_h)}, \quad (20)$$

$$R_h^{n+1} = \frac{R_h^n + h(\gamma I_h^n + \tau Q_h^n)}{1+h\mu_h} \quad (21)$$

$${S_r}^{n+1} = \frac{N_r{S_r}^n + hN_r\theta_r}{N_r(1+h(\beta_3{I_r}^n + N_r\mu_r))}, \quad (22)$$

$${E_r}^{n+1} = \frac{N_r{E_r}^n + h(\beta_3{S_r}^n{I_r}^n)}{N_r(1+h(\mu_r+\alpha_3))}, \quad (23)$$

$${I_r}^{n+1} = \frac{{I_r}^n + h\alpha_3{E_r}^n}{1+h(\mu_r+\delta_r)}. \quad (24)$$

C. *Positivity of NSFD Scheme*

Theorem 1. *Let the state variables* $S_h(t), E_h(t), I_h(t), Q_h(t), R_h(t), S_r(t), E_r(t)$, *and* $I_r(t)$ *be positive at* $t = 0$. *Also, let* $\theta_h, \theta_r, \beta_1, \beta_2, \beta_3, \alpha_1, \alpha_2, \alpha_3, \varphi, \tau, \gamma, \mu_h, \mu_r, \delta_r$, *and* δ_h *be positive in the model. Then,*

$$S_h^{n+1} \geq 0, \quad E_h^{n+1} \geq 0, \quad I_h^{n+1} \geq 0, \quad Q_h^{n+1} \geq 0, \quad R_h^{n+1} \geq 0, \quad S_r^{n+1} \geq 0, \quad E_r^{n+1} \geq 0, \quad I_r^{n+1} \geq 0.$$

Proof: By substituting $n = 0$ into the system (17-24), we derive the following expression.

$${S_h}^1 = \frac{{S_h}^0 N_h + hN_h(\varphi{Q_h}^0 + \theta_h)}{N_h + h\mu_h N_h + h(\beta_1{I_r}^0 + \beta_2{I_h}^0)} \geq 0,$$

$${E_h}^1 = \frac{N_h{E_h}^0 + h(\beta_1{I_r}^0 + \beta_2{I_h}^0){S_h}^0}{N_h(1+h(\alpha_1+\alpha_2+\mu_h))} \geq 0,$$

$${I_h}^1 = \frac{{I_h}^0 + h\alpha_1{E_h}^0}{1+h(\mu_h+\delta_h+\gamma)} \geq 0,$$

$${Q_h}^1 = \frac{{Q_h}^0 + h\alpha_2{E_h}^0}{1+h(\varphi+\tau+\mu_h+\delta_h)} \geq 0,$$

$${R_h}^1 = \frac{{R_h}^0 + h(\gamma{I_h}^0 + \tau{Q_h}^0)}{1+h\mu_h} \geq 0,$$

$$S_r{}^1 = \frac{N_r S_r{}^0 + hN_r\theta_r}{N_r(1+h\left(\beta_3 I_r{}^0 + N_r\mu_r\right))} \geq 0,$$

$$E_r{}^1 = \frac{N_r E_r{}^0 + h(\beta_3 S_r{}^0 I_r{}^0)}{N_r(1+h\left(\mu_r+\alpha_3\right))} \geq 0,$$

$$I_r{}^1 = \frac{I_r{}^0 + h\alpha_3\, E_r{}^0}{1+h\left(\mu_r+\delta_r\right)} \geq 0.$$

Now, by substituting $n = 1$ into the system (17-24) to reach the following step,

$$S_h{}^2 = \frac{S_h{}^1 N_h + hN_h(\varphi Q_h{}^1 + \theta_h)}{N_h + h\mu_h N_h + h(\beta_1 I_r{}^1 + \beta_2 I_h{}^1)} \geq 0,$$

$$E_h{}^2 = \frac{N_h E_h{}^1 + h(\beta_1 I_r{}^1 + \beta_2 I_h{}^1) S_h{}^1}{N_h\left(1+h\left(\alpha_1+\alpha_2+\mu_h\right)\right)} \geq 0,$$

$$I_h{}^2 = \frac{I_h{}^1 + h\alpha_1 E_h{}^1}{1+h(\mu_h+\delta_h+\gamma)} \geq 0,$$

$$Q_h{}^2 = \frac{Q_h{}^1 + h\alpha_2 E_h{}^1}{1+h(\varphi+\tau+\mu_h+\delta_h)} \geq 0,$$

$$R_h{}^2 = \frac{R_h{}^1 + h(\gamma I_h{}^1 + \tau Q_h{}^1)}{1+h\mu_h} \geq 0,$$

$$S_r{}^2 = \frac{N_r S_r{}^1 + hN_r\theta_r}{N_r(1+h\left(\beta_3 I_r{}^1 + N_r\mu_r\right))} \geq 0,$$

$$E_r{}^2 = \frac{N_r E_r{}^1 + h(\beta_3 S_r{}^1 I_r{}^1)}{N_r(1+h\left(\mu_r+\alpha_3\right))} \geq 0,$$

$$I_r{}^2 = \frac{I_r{}^1 + h\alpha_3\, E_r{}^1}{1+h\left(\mu_r+\delta_r\right)} \geq 0.$$

Next, let's assume that the aforementioned system of equations guarantees that the variables maintain positivity attributes for for $n = 2,\ 3,\ 4, \ldots,\ n-1$, i.e., ${S_h}^{n+1} \geq 0,\ {E_h}^{n+1} \geq 0,\ {I_h}^{n+1} \geq 0,\ {Q_h}^{n+1} \geq 0, {R_h}^{n+1} \geq 0, {S_r}^{n+1} \geq 0, {E_r}^{n+1} \geq 0, {I_r}^{n+1} \geq 0$; for $n = 2,\ 3,\ 4, \ldots,\ n-1$.

Now, let's examine the positivity for a randomly chosen positive integer $n \in \mathbb{Z}$, we observe that

$$S_h{}^{n+1} = \frac{S_h{}^n N_h + hN_h(\varphi Q_h{}^n + \theta_h)}{N_h + h\mu_h N_h + h(\beta_1 I_r{}^n + \beta_2 I_h{}^n)} \geq 0,$$

$$E_h{}^{n+1} = \frac{N_h E_h{}^n + h(\beta_1 I_r{}^n + \beta_2 I_h{}^n) S_h{}^n}{N_h(1+h\left(\alpha_1+\alpha_2+\mu_h\right))} \geq 0,$$

$$I_h{}^{n+1} = \frac{I_h{}^n + h\alpha_1 E_h{}^n}{1+h(\mu_h+\delta_h+\gamma)} \geq 0,$$

$$Q_h{}^{n+1} = \frac{Q_h{}^n + h\alpha_2 E_h{}^n}{1+h(\varphi+\tau+\mu_h+\delta_h)} \geq 0,$$

$$R_h{}^{n+1} = \frac{R_h{}^n + h(\gamma I_h{}^n + \tau Q_h{}^n)}{1+h\mu_h} \geq 0,$$

$$S_r{}^{n+1} = \frac{N_r S_r{}^n + hN_r\theta_r}{N_r(1+h\left(\beta_3 I_r{}^n + N_r\mu_r\right))} \geq 0,$$

$$E_r{}^{n+1} = \frac{N_r E_r{}^n + h(\beta_3 S_r{}^n I_r{}^n)}{N_r(1+h\left(\mu_r+\alpha_3\right))} \geq 0,$$

$$I_r{}^{n+1} = \frac{I_r{}^n + h\alpha_3\, E_r{}^n}{1+h\left(\mu_r+\delta_r\right)} \geq 0.$$

Consequently, the proposed scheme ensures the positivity of the state variables for all positive integer values of n.

D. Consistency Analysis

In this section, we conduct a consistency analysis of the system (17-24) scheme using Taylor's series expansion (TSE). The TSE of ${S_h}^{n+1}$ is calculated as follows:

$$S_h{}^{n+1} = S_h{}^n + h\frac{dS_h}{dt} + \frac{h^2}{2!}\frac{d^2S_h}{dt^2} + \frac{h^3}{3!}\frac{d^3S_h}{dt^3} + \ldots,$$

From the first equation of the NSFD scheme, we have

$$S_h{}^{n+1}\left(N_h + h\mu_h N_h + h(\beta_1 I_r{}^n + \beta_2 I_h{}^n)\right) = S_h{}^n N_h + hN_h(\varphi Q_h{}^n + \theta_h).$$

Substituting the value of ${S_h}^{n+1}$ in the above equation, we obtain

$$\left(S_h^n + h\tfrac{dS_h}{dt} + \tfrac{h^2}{2!}\tfrac{d^2S_h}{dt^2} + \tfrac{h^3}{3!}\tfrac{d^3S_h}{dt^3} + \ldots\right)\left(N_h + h\mu_h N_h + h\left(\beta_1 I_r^n + \beta_2 I_h^n\right)\right) = S_h^n N_h + hN_h\left(\varphi Q_h^n + \theta_h\right)$$

After some simplification and applying $h \longrightarrow 0$, we obtain

$$\frac{dS_h}{dt} = \theta_h - \frac{(\beta_1 I_r + \beta_2 I_h) S_h}{N_h} - \mu_h S_h + \varphi Q_h.$$

This finding indicates that our discretized equation is in line with the equation of system (1-8). Similarly, by examining the second equation of the system (17-24), we arrive at

$${E_h}^{n+1}(N_h\left(1+h\left(\alpha_1+\alpha_2+\mu_h\right)\right) = N_h {E_h}^n + h(\beta_1 {I_r}^n + \beta_2 {I_h}^n){S_h}^n.$$

$$\Rightarrow \frac{dE_h}{dt} = \frac{(\beta_1 I_r + \beta_2 I_h) S_h}{N_h} - \left(\alpha_1+\alpha_2+\mu_h\right) E_h.$$

Similarly, substituting the value of ${I_h}^{n+1}$ in the third equation of the system (17-24), we obtain as follows

$$\left(I_h^n + h\tfrac{dI_h}{dt} + \tfrac{h^2}{2!}\tfrac{d^2I_h}{dt^2} + \tfrac{h^3}{3!}\tfrac{d^3I_h}{dt^3} + \ldots\right)\left(1+h\left(\mu_h+\delta_h+\gamma\right)\right) = I_h^n + h\alpha_1 E_h^n,$$

$$\Rightarrow \frac{dI_h}{dt} = \alpha_1 E_h - \left(\mu_h+\delta_h+\gamma\right) I_h.$$

On a similar pattern, applying Taylor's series expansion of ${Q_h}^{n+1}$, ${R_h}^{n+1}$, ${S_r}^{n+1}$, ${E_r}^{n+1}$, and ${I_r}^{n+1}$ in the fourth, fifth, sixth, seventh and last equation of the system (3), and simplifying we obtain as follows

$$\frac{dQ_h}{dt} = \alpha_2 E_h - \left(\varphi+\tau+\mu_h+\delta_h\right) Q_h,$$

$$\frac{dR_h}{dt} = (\gamma I_h + \tau Q_h) - R_h\mu_h,$$

$$\frac{dS_r}{dt} = \theta_r - S_r\left(\beta_3 I_r + N_r\mu_r\right),$$

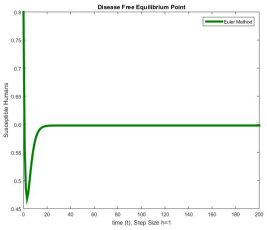

(a) Susceptible humans at $h = 1$

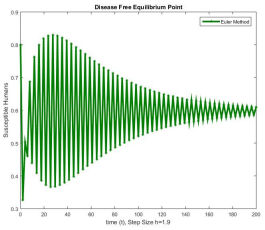

(b) Susceptible humans at $h = 1.9$

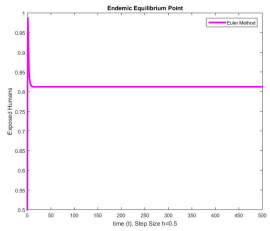

(c) Infected humans at $h = 1$

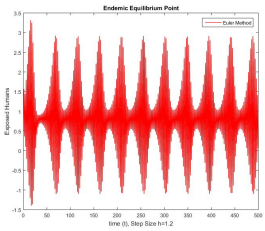

(d) Infected humans at $h = 2$

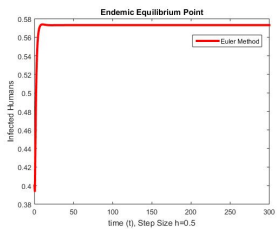

(e) exposed humans at $h = 1$

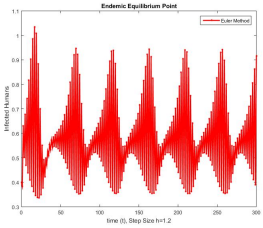

(f) exposed humans at $h = 2$

Figure 2: Susceptible, Infected and exposed humans using the Euler scheme at DFE

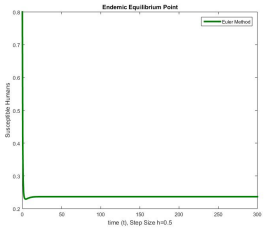

(a) Susceptible humans at $h = 1$

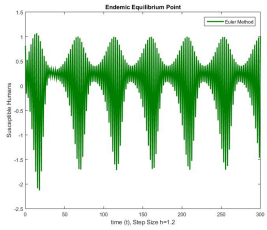

(b) Susceptible humans at $h = 2$

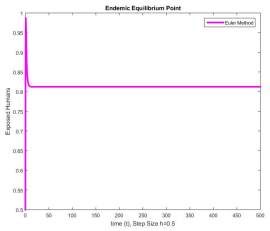

(c) Infected humans at $h = 1$

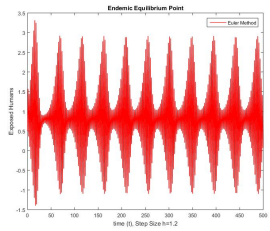

(d) Infected humans at $h = 2$

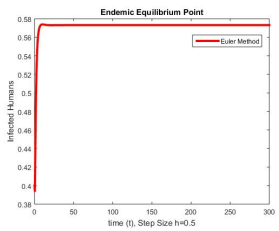

(e) exposed humans at $h = 1$

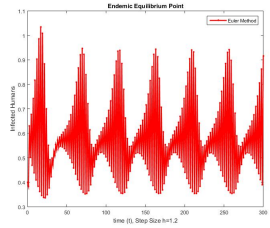

(f) exposed humans at $h = 2$

Figure 3: Susceptible, Infected and exposed humans using the Euler scheme at EE

$$\frac{dE_r}{dt} = (\beta_3 S_r I_r) - E_r\left(\mu_r + \alpha_3\right),$$

$$\frac{dI_r}{dt} = \alpha_3\, E_r - I_r\left(\mu_r + \delta_r\right).$$

Thus, our discretized implicit numerical integration scheme aligns with the equations of the system (1-8).

4. Results and Discussions

In this section, numerical simulation will be employed to illustrate the performance of both the forward Euler method and the suggested NSFD scheme.

Figures 2 and 3 illustrate the graphical trends of the human sub-populations using the Euler method, observed at the DFE and EE points for various step size values. The Euler approach demonstrates convergence at smaller step sizes but starts exhibiting non-physical oscillations and generating negative values as the step size increases. Negative values in these contexts hold no meaningful interpretation, as populations cannot be negative. This behavior depicted by the graphs indicates that the Euler method is inadequate for accurately representing the dynamics of MPX disease. Figures 4 and 5 showcase the graphical trajectories of the human sub-populations utilizing the NSFD method, observed at the DFE and EE points across various step size values. Notably, the NSFD scheme consistently maintains positivity and convergence regardless of changes in step size. This indicates that the NSFD scheme serves as a robust and reliable approach for depicting the dynamics of MPX virus disease. Figure 6 illustrates the effects of α_1 and α_2. It is evident that α_1 demonstrates a direct proportionality to infection; an increase in α_1 corresponds to increased infection, and vice versa. Conversely, α_2 exhibits an inverse proportionality to infection; an increase in α_2 leads to decreased infection, and vice versa. From this observation, it can be concluded that preventing exposed humans from contracting the infection is the most effective approach for reducing MPX virus disease.

5. Conclusion

After the eradication of smallpox, monkeypox has become the most well-known Orthopoxvirus zoonosis. The disease is caused by the monkeypox virus, a phylogenetically related zoonotic agent originating from rodents, found in various Central and West African countries. Monkeypox results in a severe, highly infectious, and incapacitating illness, posing a significant public health challenge. To effectively control future outbreaks, it is crucial to implement at least three

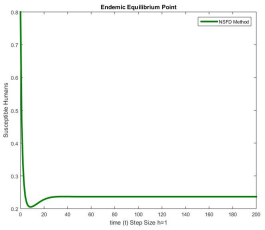

(a) Susceptible humans at $h = 1$

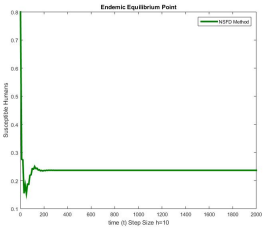

(b) Susceptible humans at $h = 10$

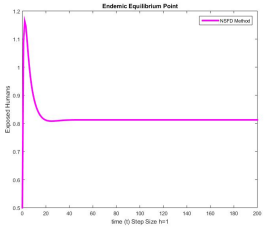

(c) Infected humans at $h = 1$

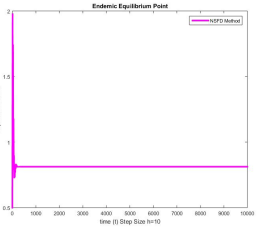

(d) Infected humans at $h = 10$

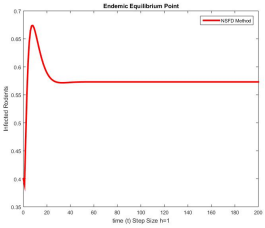

(e) exposed humans at $h = 1$

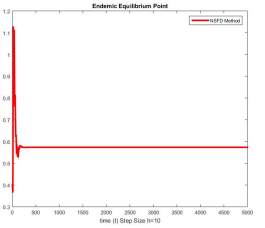

(f) exposed humans at $h = 10$

Figure 4: Susceptible, Infected and exposed humans using the NSFD scheme at DFE

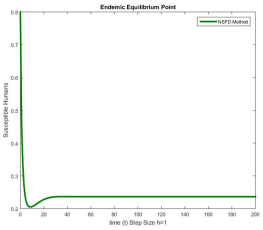

(a) Susceptible humans at $h = 1$

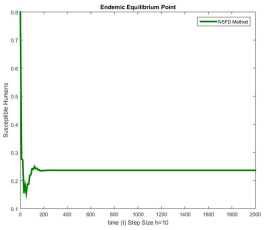

(b) Susceptible humans at $h = 10$

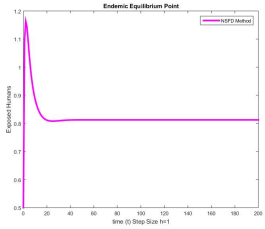

(c) Infected humans at $h = 1$

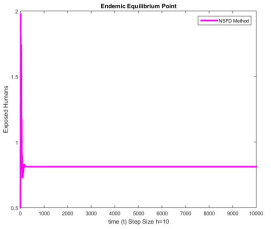

(d) Infected humans at $h = 10$

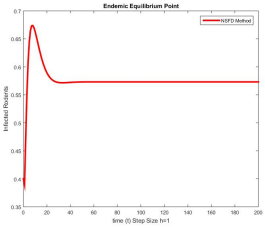

(e) exposed humans at $h = 1$

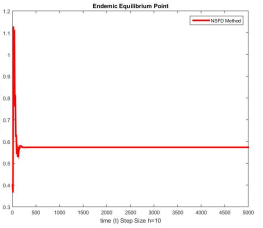

(f) exposed humans at $h = 10$

Figure 5: Susceptible, Infected and exposed humans using the NSFD scheme at EE

prevention strategies: preventive vaccination in humans, environmental management, and disease surveillance.

Mathematical modeling has become an indispensable guide for planning, executing, and tracking diseases during epidemics and pandemics scientifically. The role of various surveillance and tracking organizations through mathematical modeling has become pertinent in recent years. Mathematical modeling is easily recognized in protocol design and has advantages in logistical problem-solving. It is also considered valuable in the design of epidemiological tools, especially in data collection methods and interpretation of the data, not only collected but also for the initial stage analysis.

In this study, we considered and analyzed an epidemiological model depicting the transmission dynamics of MPX disease to understand the transmission dynamics of MPX disease. The proposed model comprises eight mutually exclusive compartments. The human population has been divided into four compartments: exposed individuals, isolated humans, infected humans, and recovered humans. Just as humans are categorized into three groups, rats are also classified into exposed, susceptible, and infected rodents. The sensitivity analysis of the reproduction number revealed that β_2, representing the human-to-human contact rate, is the most

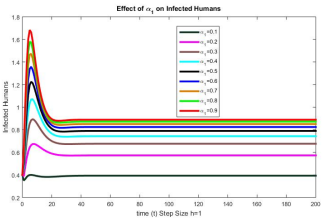

(a)

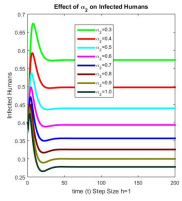

(b)

Figure 6: Effect of α_1 and α_2 on infected humans

sensitive parameter in the transmission of the disease. Additionally, α_1 the ratio of exposed humans becoming infected, was found to significantly influence the propagation of MPX disease within host populations. The results emphasize the importance of decreasing human-to-human contact rates to effectively control the spread of MPX disease within the population. This underscores the need for healthcare professionals and policymakers to prioritize interventions aimed at addressing this aspect.

Considering the challenges related to controlling rodent populations, the most effective strategy for preventing, mitigating, and controlling MPX disease involves minimizing

contact with infected individuals.

This can be accomplished by promoting vaccination against MPX infection in highly endemic regions as an additional preventive measure, as well as by educating the public about the disease, encouraging good personal hygiene habits, sterilizing medical equipment, and using personal protective equipment when caring for infected individuals.

Two different strategies are used to solve the problem numerically, and the resulting graphical representations of each method are compared. The simulation shows that even at very small step sizes, the Euler technique is unable to produce findings that can be trusted. In contrast, the suggested approach delivers precise and convergent outcomes across all chosen step size values. Furthermore, the NSFD scheme's positivity, boundedness, and consistency are scrutinized. This scheme upholds positivity, a pivotal attribute given that model compartments represent populations that cannot exhibit negative values. Consequently, negative values hold no relevance in such models. On occasion, the Euler method generates negative values with specific step size selections, making it inadequate for investigating disease dynamics within the considered model. The investigation into the effects of α_1 and α_2 on infected humans reveals that the most effective means of reducing MPX virus disease involves preventing exposed individuals from contracting the infection. The main focus of this study lies in constructing an NSFD scheme for solving the dynamics of the MPX virus disease model. The work can be extended to fractional, fuzzy, delayed, and stochastic domains, as well as exploring additional directions.

Conflict of interest

The authors declare no conflict of interests. All authors read and approved final version of the paper.

Authors Contribution

All authors contributed equally in this paper.

References

[1] WHO. Monkeypox. WHO (2024). Available from: Available online at: https://www.who.int/en/news-room/fact-sheets/detail/monkeypox (accessed on 10 May 2024).

[2] Jezek, Z., Szczeniowski, M., Paluku, K. M., Mutombo, M., & Grab, B. (1988). Human monkeypox: confusion with chickenpox. *Acta tropica, 45*(4), 297–307.

[3] Nigeria Centre for Disease Control and Prevention. Monkeypox (2024). Available from: https://ncdc.gov.ng/diseases/info/M (accessed on 10 May 2024).

[4] Von Magnus, P., Andersen, E. K., Petersen, K. B., & Birch-Andersen, A. (2009). A pox-like disease in cynomolgus monkeys. *Acta Pathologica Microbiologica Scandinavica, 46*, 156–176.

[5] Breman, J. G., Ruti, K., & Steniowski, M. V. (1980). Human monkeypox, 1970–1979. *Bulletin of the World Health Organization, 58*, 165–182.

[6] Ladnyj, I. D., Ziegler, P., & Kima, E. (1972). A human infection caused by monkeypox virus in Basankusu Territory, Democratic Republic of the Congo. *Bulletin of the World Health Organization, 46*, 593–597.

[7] Foster, S. O., Brink, E. W., Hutchins, D. L., Pifer, J. M., Lourie, B., Moser, C. R., Cummings, E. C., Kuteyi, O. E. K., Eke, R. E. A., Titus, J. B., et al. (1972). Human monkeypox. *Bulletin of the World Health Organization, 46*, 569–576.

[8] Monkeypox. (2024). Retrieved from https://www.who.int/health-topics/monkeypox/#tab=tab_1 (accessed on 10 May 2024).

[9] CDC. (2024). Ongoing 2022 Global Outbreak Cases and Data. Retrieved from https://www.cdc.gov/poxvirus/Mpox/response/2022/world-map.html (accessed on 10 May 2024).

[10] Nolen, L. D., Osadebe, L., Katomba, J., Likofata, J., Mukadi, D., Monroe, B., ... & Reynolds, M. G. (2016). Extended human-to-human transmission during a monkeypox outbreak in the Democratic Republic of the Congo. *Emerging Infectious Diseases, 22*(6), 1014.

[11] Meyer, H., Ehmann, R., & Smith, G. L. (2020). Smallpox in the post-eradication era. *Viruses, 12*(2), 138.

[12] Rimoin, A. W., Mulembakani, P. M., Johnston, S. C., Lloyd Smith, J. O., Kisalu, N. K., Kinkela, T. L., ... & Muyembe, J. J. (2010). Major increase in human monkeypox incidence 30 years after smallpox vaccination campaigns cease in the Democratic Republic of Congo. *Proceedings of the National Academy of Sciences, 107*(37), 16262-16267.

[13] Bhunu, C., & Mushayabasa, S. (2011). Modelling the transmission dynamics of pox-like infections. *IAENG International Journal, 41*(2), 1–9.

[14] Somma, S. A., Akinwande, N. I., & Chado, U. D. (2019). A mathematical model of monkey pox virus transmission dynamics. *Ife Journal of Science, 21*(1), 195-204.

[15] Usman, S., & Adamu, I. I. (2017). Modeling the transmission dynamics of the monkeypox virus infection with treatment and vaccination interventions. *Journal of Applied Mathematics and Physics, 5*(12), 2335.

[16] Philemon, M. E., Olopade, I. A., & Ogbaji, E. O. (2023). Mathematical analysis of the effect of quarantine on the dynamical transmission of monkey pox. *Asian Journal of Pure and Applied Mathematics*, 473-492.

[17] Samuel, M. D., Woodworth, B. L., Atkinson, C. T., Hart, P. J., & LaPointe, D. A. (2018). The epidemiology of avian pox and interaction with avian malaria in Hawaiian forest birds. *Ecological Monographs, 88*(4), 621-637.

[18] Peter, O. J., Abidemi, A., Ojo, M. M., & Ayoola, T. A. (2023). Mathematical model and analysis of monkeypox with control strategies. *The European Physical Journal Plus, 138*(3), 242.

[19] Peter, O. J., Madubueze, C. E., Ojo, M. M., Oguntolu, F. A., & Ayoola, T. A. (2023). Modeling and optimal control of monkeypox with cost-effective strategies. *Modeling Earth Systems and Environment, 9*(2), 1989-2007.

[20] Khan, A., Sabbar, Y., & Din, A. (2022). Stochastic modeling of the Monkeypox 2022 epidemic with cross-infection hypothesis in a highly disturbed environment. *Mathematical Biosciences and Engineering, 19*(12), 13560-13581.

[21] Al-Shomrani, M. M., Musa, S. S., & Yusuf, A. (2023). Unfolding the transmission dynamics of monkeypox virus: an epidemiological modelling analysis. *Mathematics, 11*(5), 1121.

[22] Peter, O. J., Kumar, S., Kumari, N., Oguntolu, F. A., Oshinubi, K., & Musa, R. (2022). Transmission dynamics of Monkeypox virus: a mathematical modelling approach. *Modeling Earth Systems and Environment*, 1-12.

[23] Cadmus, S., Akinseye, V., Besong, M., Olanipekun, T., Fadele, J., Cadmus, E., ... & Tomori, O. (2024). Dynamics of Mpox infection in Nigeria: a systematic review and meta-analysis. *Scientific Reports, 14*(1), 7368.

[24] Onitilo, S., Ajani, A., Daniel, D., & Haruna, A. (2024). Mathematical Modeling of the Transmission Dynamics of Monkeypox with the Impact of Quarantine and Public Enlightenment in Nigeria. *Journal of Innovative Science and Engineering, 8*(1), 1-17.

[25] Sweilam, N. H., Mohammed, Z. N., & Kareem, W. A. (2024). Numerical approaches for solving complex order monkeypox mathematical model. *Alexandria Engineering Journal, 90*, 170-182.

[26] Alqahtani, R. T., Musa, S. S., & Inc, M. (2023). Modeling the role of public health intervention measures in halting the transmission of monkeypox virus. *AIMS Mathematics, 8*(6), 14142-14166.

[27] Mickens, R. E. (1994). *Nonstandard finite difference models of differential equations*. World Scientific.

[28] Verma, A. K., & Kayenat, S. (2018). On the convergence of Mickens' type nonstandard finite difference schemes on Lane–Emden type equations. *Journal of Mathematical Chemistry, 56*, 1667-1706.

[29] Verma, A. K., & Kayenat, S. (2019). On the stability of Micken's type NSFD schemes for generalized Burgers Fisher equation. *Journal of Difference Equations and Applications, 25*(12), 1706-1737.

[30] Verma, A. K., Pandit, B., Verma, L., & Agarwal, R. P. (2020). A review on a class of second order nonlinear singular BVPs. *Mathematics, 8*(7), 1045.

[31] Raza, A., Rafiq, M., Baleanu, D., Arif, M. S., Naveed, M., et al. (2019). Competitive numerical analysis for stochastic HIV/AIDS epidemic model in a two-sex population. *IET Systems Biology, 13*(6), 305-315.

[32] Iqbal, Z., Ahmed, N., Baleanu, D., Adel, W., Rafiq, M., et al. (2020). Positivity and boundedness preserving numerical algorithm for the solution of fractional nonlinear epidemic model of HIV/AIDS transmission. *Chaos, Solitons & Fractals, 134*(1), 109706.

[33] Ahmed, N., Rafiq, M., Adel, W., Rezazadeh, H., Khan, I., et al. (2020). Structure preserving numerical analysis of HIV and CD4+ T-cells reaction diffusion model in two space dimensions. *Chaos, Solitons & Fractals, 139*(1), 110307.

[34] Allehiany, F. M., Dayan, F., Al-Harbi, F. F., Althobaiti, N., Ahmed, N., et al. (2022). Bio-inspired numerical analysis of COVID-19 with fuzzy parameters. *Computers, Materials & Continua, 72*(2), 3213-3229.

[35] Verma, A. K., & Kayenat, S. (2020). An efficient Mickens' type NSFD scheme for the generalized Burgers Huxley equation. *Journal of Difference Equations and Applications, 26*(9-10), 1213-1246.

[36] Chitnis, N., Hyman, J. M., & Cushing, J. M. (2008). Determining important parameters in the spread of malaria through the sensitivity analysis of a mathematical model. *Bulletin of Mathematical Biology, 70*, 1272-1296.